Langmuir–Blodgett Film Formed by Amphiphilic Molecules for Facile and Rapid Construction of Zinc–Iodine Cell

Leiqian Zhang, Jiale Ge, Tianlu Wang, Hele Guo, Suli Chen, Yue-E Miao, Elke Debroye, Guanjie He, Ivan P. Parkin, Johan Hofkens, Feili Lai, and Tianxi Liu**

L. Q. Zhang, J. L. Ge, T. L. Wang, S. L. Chen, Prof. T. X. Liu
Key Laboratory of Synthetic and Biological Colloids, Ministry of Education, School of Chemical and Material Engineering, International Joint Research Laboratory for Nano Energy Composites, Jiangnan University, Wuxi, 214122, P. R. China

H. L. Guo, Prof. E. Debroye, Prof. J. Hofkens, Dr. F. L. Lai
Department of Chemistry, KU Leuven, Celestijnenlaan 200F, Leuven 3001, Belgium

Prof. Y. E. Miao
State Key Laboratory for Modification of Chemical Fibers and Polymer Materials, College of Materials Science and Engineering, Donghua University, Shanghai, 201620 P. R. China

Prof. G. J. He, Prof. I. P. Parkin
Department of Chemistry, University College London, London, WC1H 0AJ, United Kingdom

Prof. J. Hofkens
Department of Molecular Spectroscopy, Max Planck Institute for Polymer Research, Ackermannweg 10, Mainz 55128, Germany

Dr. F. L. Lai
State Key Laboratory of Metal Matrix Composites, School of Materials Science and Engineering, Shanghai Jiao Tong University, Shanghai, 200240, P. R. China

***Corresponding Author**

E-mail: feili.lai@kuleuven.be and feililai@sjtu.edu.cn
E-mail: txliu@jiangnan.edu.cn

KEYWORDS: zinc-iodine battery, fast construction, Langmuir-Blodgett film, amphiphilic molecule

ABSTRACT: Zinc-iodine batteries (ZIBs) are promising candidates for ecofriendly, safe, and low-cost energy storage systems, but polyiodide shuttling and the complex cathode fabrication procedures have severely hindered their broader commercial usage. Herein, a protocol is developed, using phospholipid-like oleylamine molecules for scalable production of Langmuir-Blodgett films, which allows the facile preparation of ZIB cathodes in less than 1 min. The resulting inhomogeneous cathode allows for the continuous conversion of iodine. Moreover, the amine group of the oleylamine molecule at the cathode is capable of producing $[OA^*I^+]I_3^-$ charge-transfer complexes with iodine, which facilitates the rapid migration of iodine and results in a highly reversible iodine conversion process. Consequently, the as-prepared ZIBs can deliver over 2000 cycles at 0.5 mA cm^{-2} with a capacity retention of 75.3%. This work presents a novel, straightforward, and efficient method for the rapid construction of ZIBs.

TOC GRAPHICS

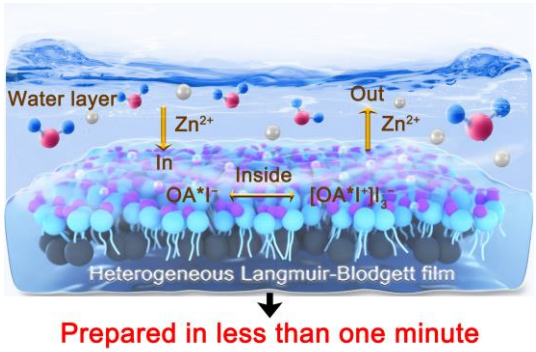

Rechargeable zinc metal batteries (RZMBs) that utilize neutral and slightly acidic aqueous electrolytes have garnered significant attention in recent years.[1-5] This can primarily be attributed to their unique advantages, including superior security, ecofriendly, low manufacturing cost, and high specific capacity, which fulfill the current requirements for grid-scale electrochemical energy storage (EES) systems.[2,6-11] Among the numerous cathode materials available for RZMBs, iodine has recently come into the research limelight.[12-14] This is due to the highly reversible conversion process of iodine, which provides a suitable voltage platform of ~1.3 V for RZMBs to prevent the oxygen evolution reaction, as well as a high theoretical specific capacity of ~211 mAh g^{-1}.[15-17] Additionally, the affordability and abundance of iodine make zinc-iodine batteries (ZIBs) promising for implementation in the field of large-scale EES systems.[18,19]

However, the detrimental shuttle effect arising from the dissolution and diffusion of polyiodide in aqueous electrolytes typically leads to the short lifetime and rapid self-discharge of battery, which greatly hinder the widespread adoption of ZIBs.[16,20,21] Several iodine host materials, including carbon matrices,[19] organic polymers,[18] MXenes,[22] and Prussian blue analogues,[23] have been explored to temper the polyiodide shuttling for achieving highly stable ZIBs. Notably, the construction of composite cathodes from these materials with iodine usually requires a tedious and complicated procedure. It involves the following stages: loading iodine into host materials, preparing slurries with iodine, applying the slurries onto current collectors, and drying the cathode sheets. Such time-consuming steps undeniably hinder the widespread application of ZIBs in EES systems. Therefore, the creation of iodine cathodes that can be produced rapidly and prevent polyiodide shuttling would be an essential

component in accelerating the usability of ZIBs.

In order to fabricate such cathodes, the iodine host material may possess a set of essential attributes. These characteristics include: 1) rapid iodine capture through electrochemical charging to avoid additional iodine loading processes (e.g., infiltration and sublimation); 2) effective immobilization of captured iodine species to mitigate polyiodide shuttling; 3) suitable viscosity to facilitate integration onto current collectors; 4) insolubility in water to prevent potential cathode dissolution issues. Notably, small amphiphilic molecules may meet these bespoke requirements. Their long-chain hydrophobic tails prevent them from dissolving in water, while the hydrophilic heads contain appropriate functional groups capable of trapping and confining polyiodide during charging.[18] Moreover, due to their distinctive molecular structure, these molecules possess a remarkable capability to spread spontaneously across the water surface and form a well-known Langmuir film.[24-26] Meanwhile, this Langmuir film can be integrated directly onto the current collector, as it possesses an appropriate viscosity derived from its long-chain alkane structure.[27] Consequently, Langmuir-Blodgett (films can be created and serve as a viable electrode material for batteries.[28,29] Hence, small amphiphilic molecules present an ideal solution for swiftly establishing cost-effective, environmentally friendly, and highly scalable ZIBs. To date, little is known about the application of LB films in ZIB systems, necessitating urgent and comprehensive research efforts.

In this study, we present a novel approach to swiftly fabricate the cathodes for zinc-iodine batteries based on LB films formed by the spontaneous “oil-on-water spreading” property of oleylamine. The as-prepared cathode eliminates various labor-intensive steps involved in

traditional cathode preparation, such as pulping, coating, and drying, which can significantly reduce the lead time for cathode production to less than 1 min. Additionally, this cathode allows for stable and continuous conversion of the absorbed iodine within it, as the amine groups of oleylamine can interact with iodine species to inhibit the shuttle effect and achieve ionization of iodine for promoting the iodine redox chemistry at the cathode. As a result, cells designed utilizing the LB film realize excellent cyclability with a capacity retention of 75.3% at 0.5 mA cm^{-1} after 2000 cycles. These findings demonstrate the feasibility of using amphiphilic molecules for the rapid construction of ZIB cathodes.

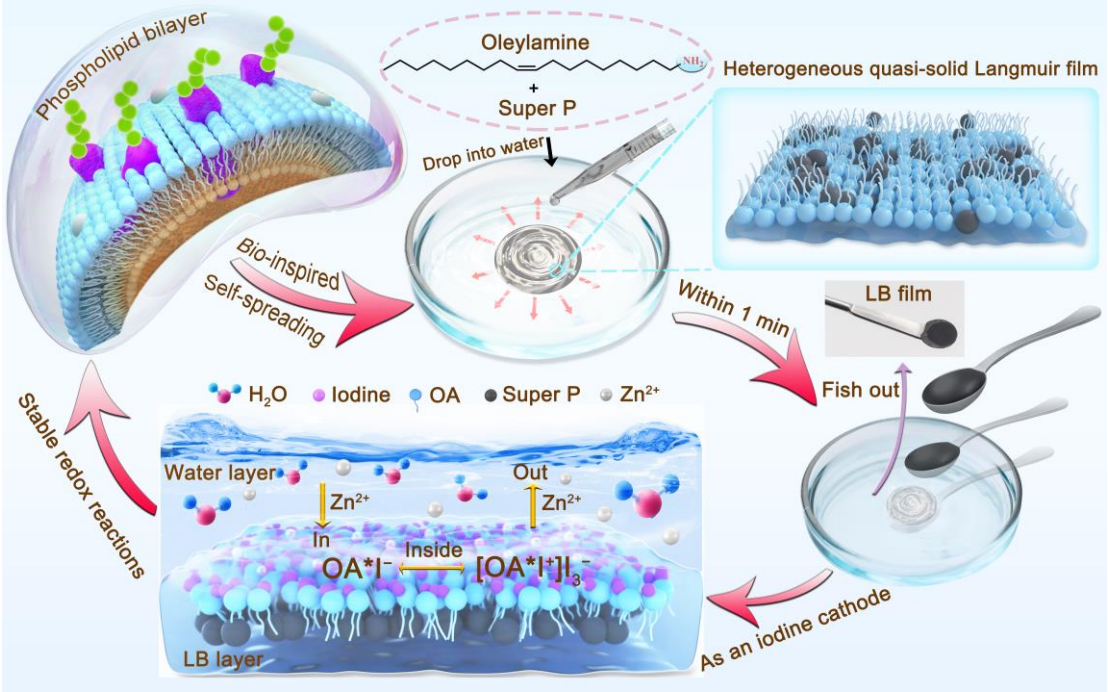

Figure 1. Schematic diagram of the phospholipid bilayer-inspired preparation of a heterogeneous LB film for ZIBs.

Figure 1 presents a schematic diagram to illustrate the process for preparing the LB film. Molecules featuring hydrophilic heads and hydrophobic tails spread on the water surface smoothly, forming Langmuir films in response to the surface tension gradient across the liquid-air interface.[30] One example of such molecules is phospholipids that can self-assemble

into a double-layered structure (known as the phospholipid bilayer). These bilayers serve as fundamental scaffold of cell membranes, playing a crucial role in maintaining a stable metabolic environment within the cell while regulating substance transport both into and out of the cell. Interestingly, this bears similarities to the iodine conversion process occurring in a cathode, where iodine reacts stably within the cathode while ions (e.g., Zn^{2+}) pass through it. Furthermore, LB films are obtained by transferring Langmuir films from the air/water interface onto a solid substrate, such as carbon paper.[28] In light of this, we first leveraged the self-spreading behavior of oleylamine (OA) on water surface to form quasi-solid Langmuir films for efficient preparation of cathodes in ZIBs. In detail, a Super P conductive agent was introduced into the OA to ensure effective electron transport. When the content of the conductive agent increases, however, the adhesiveness heightens and impedes the spreading of the oleylamine/Super P (OA/C) layer (Figure S1). Therefore, a mass ratio of 40: 1 of OA to Super P was selected to create a layer with both desirable conductivity and film-forming property. Notably, Super P primarily enhances the electronic conductivity of electrodes; its usage alone in an electrolyte containing KI cannot enable charging beyond 1.6 V due to the prevalent polyiodide shuttling issue (Figure S2). Subsequently, the mixture was dropped onto deionized water to generate film exploiting the physicochemical properties (e.g., liquid, amphiphilic nature) of OA. Within 1 min, the droplet of OA/C spread across the water surface swiftly and resulted in the uniform formation of a Langmuir film (Figure S3). After using carbon paper as a current collector to retrieve the formed film, LB film can be obtained.

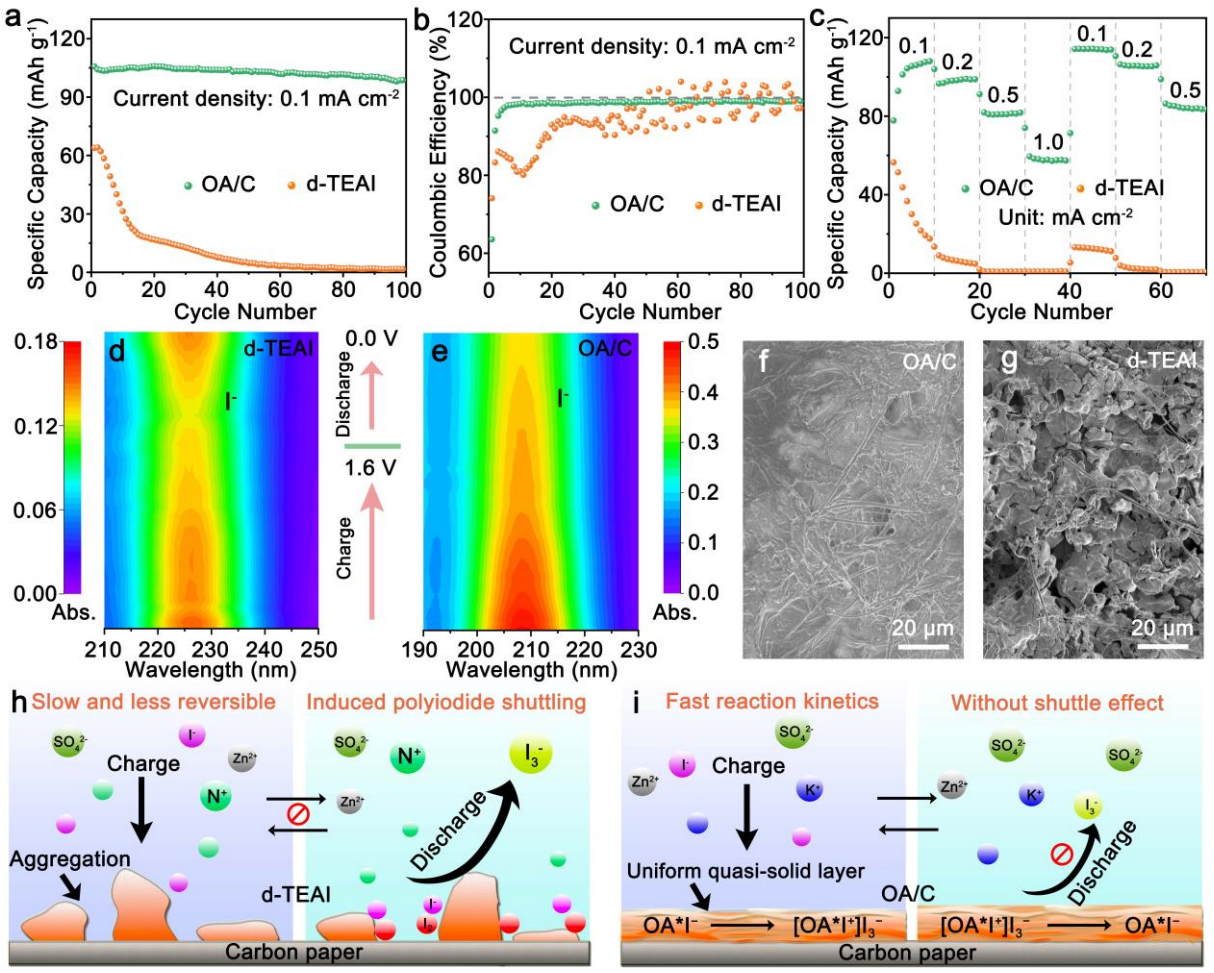

Figure 2. a) Cycle performance, and b) the corresponding CE of OA/C and d-TEAI cathodes at 0.1 mA cm^{-2}. c) Rate performance of OA/C and d-TEAI cathodes at different current densities. In situ UV-vis detection for iodine ion changes in ZIBs using d) d-TEAI, and e) OA/C cathodes during charging/discharging. SEM images of f) OA/C, and g) d-TEAI after 10 cycles at 0.1 mA cm^{-2}. Schematic comparison of h) solid d-TEAI cathode (TEA^+ is represented by N^+), and i) quasi-solid OA/C layer during the cycling process.

The electrochemical performance of the LB film was assessed within the ZIB system. For comparison, tetraethylammonium iodide (TEAI) was employed, as it can react with polyiodide to form a precipitate and inhibit the free migration of polyiodide (Figure S4). Especially, the resulting deposition-type cathode is referred to as d-TEAI. As depicted in

Figure 2a, the OA/C cathode provides a high reversible capacity of 98.7 mAh g^{-1} (corresponding to 93.4% capacity retention) after 100 cycles at 0.1 mA cm^{-2}, when employing 0.1 M KI as the iodine source (avoiding additional iodine loading process). Conversely, with the use of the d-TEAI electrode, the battery starts with an initial specific capacity as low as 63.9 mAh g^{-1} and experiences a rapid capacity drop (3% capacity retention after 100 cycles). Figure 2b also demonstrates that the OA/C cathode possesses a higher and more stable Coulombic efficiency (CE) (average: 98.25%) compared to the d-TEAI cathode (average: 94.13%), suggesting a highly reversible iodine conversion reaction within the OA/C cathode. The disparity in rate performance between d-TEAI and OA/C cathodes is further elucidated in Figure 2c. Specifically, at 1 mA cm^{-2}, the OA/C cathode achieves a specific capacity of 59.5 mAh g^{-1}, while the d-TEAI cathode exhibits nearly negligible capacity even at 0.5 A cm^{-2}, underscoring the fast kinetics within the quasi-solid OA/C cathode. Importantly, after the applied current is successively reversed back to 0.1, 0.2, and 0.5 mA cm^{-2}, the specific capacities of the OA/C cathode are capable of recovering to their initial levels entirely, whereas d-TEAI exhibits limited reversibility.

The underlying causes of the difference between OA/C and d-TEAI cathodes were further investigated. The I^- concentration in both TEAI-based (Figure 2d) and OA/C-based (Figure 2e) systems tends to decrease during charging, as the I^- in aqueous electrolyte can be oxidized to iodine in the cathode at this stage. Upon discharge, however, the I^- concentration in TEAI-based ZIBs tends to increase because TEAI is soluble in water when unbound to iodine. Given that I^- ions can combine with iodine rapidly to produce water-soluble polyiodide,[31] this will potentially induce the polyiodide shuttling in ZIBs (Figure S5a). On the contrary, in

OA/C-based ZIBs, the I^- concentration continues to reduce during discharging (Figure 2e), without detection of the signal of polyiodide (Figure S5b). This may be attributed to the excellent adsorption capacity of OA/C layer for iodine species, which allows for a redox cycling behavior of iodine species within the layer and results in stable operation of ZIBs. Scanning electron microscopy (SEM) was employed to investigate the cathode morphology after cycling. Benefiting from the quasi-solid properties of OA/C cathode, it displays a uniform and flat morphology (Figure 2f). On the other hand, the d-TEAI cathode appears stacked with an irregular surface (Figure 2g). Energy dispersive X-ray spectroscopy (EDS) mapping reveals the homogeneous distribution of iodine in the OA/C cathode (Figure S6a&b). Nevertheless, the iodine distribution in the d-TEAI cathode shows obvious aggregations with the precipitation of TEAI-iodine complex (Figure S6c&d). This could result in the inability of iodine to contact the current collector, leading to poor battery performance. Besides, the amine groups in the OA molecules are capable of forming charge-transfer complexes with iodine, as described in Equations (1) and (2).[32,33]

$$OA + I_2 \leftrightarrow [OA^*I^+]I^- \quad (1)$$

$$[OA^*I^+]I^- + I_2 \leftrightarrow [OA^*I^+]I_3^- \quad (2)$$

This phenomenon is further supported by Figure S7, where the UV-vis spectrum mainly shows the peak corresponding to polyiodide after the addition of iodine into the OA solution.[32] Moreover, these charge-transfer complexes will assist in promoting a rapid redox of iodine in OA, as the generated polyiodide can readily migrate within the cathode rapidly.[34] As illustrated in Figure S8a, a substantial enhancement (an impressive 3 orders of magnitude increase from 0.01 to 41.36 μs cm^{-1}) in the ionic conductivity of OA can be observed upon

the addition of iodine, which provides direct evidence for the high mobility of iodine species in charge-transfer complexes. When iodine is introduced to TEAI, however, the ionic conductivity is quite low (0.06 μs cm^{-1}) due to the restricted freedom of polyiodide (Figure S8a&b). Thus, the poor performance of the d-TEAI electrode can be attributed to its tendency to aggregate and the inability of iodine to migrate (i.e., no access to the current collector), as well as to polyiodide shuttling induced by the dissolution of TEAI in the electrolyte (Figure 2h). In contrast, the OA/C layer enables a swift and fully reversible redox process of iodine, thanks to its quasi-solid nature with shuttle-free and highly mobile polyiodide ions (Figure 2i). Benefiting from this, zinc ions show reversible migration in and out of the OA/C cathode during charging/discharging processes (Figure S9a-f). Besides, ex-situ X-ray photoelectron spectroscopy demonstrates a reversible conversion from I^- to I^0 in the OA/C cathode (Figure S10).[35,36]

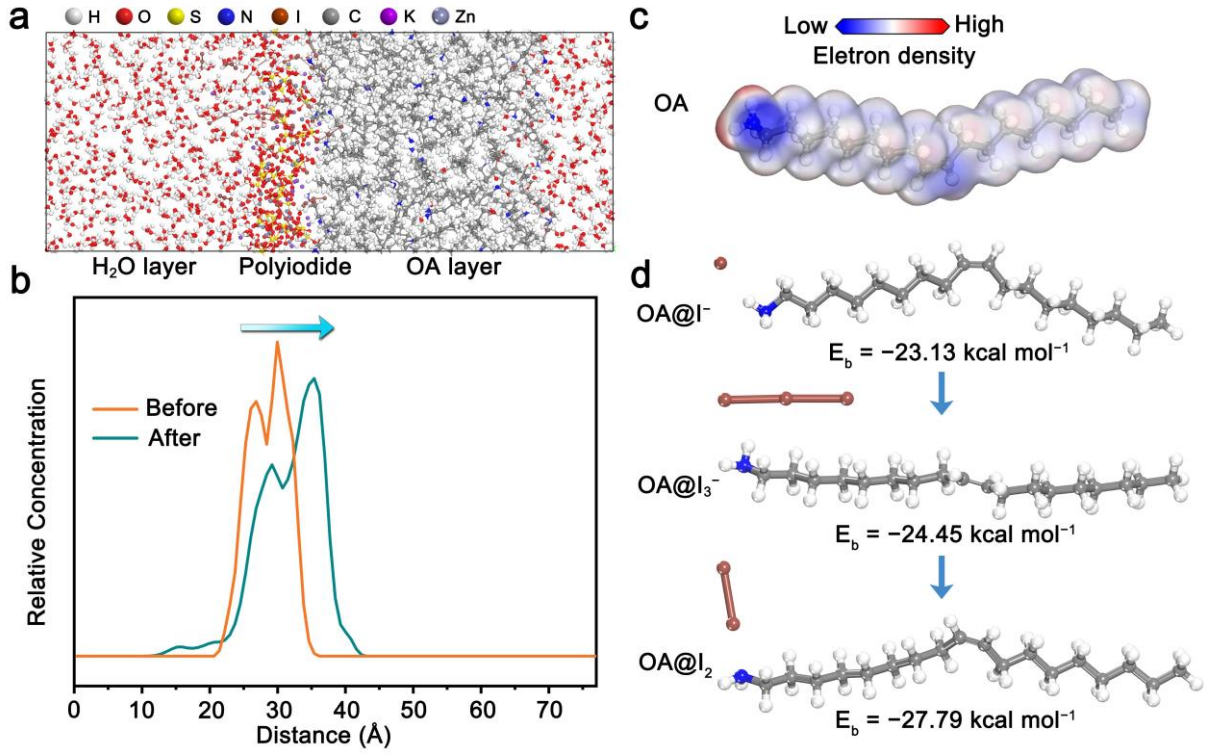

Figure 3. a) MD structural model comparing the affinities of water and the OA layer for

polyiodide. b) Distributions of polyiodide in MD structures before and after diffusion. The water molecule layer ranges from 0 to 30 Å along the X-axis, while the OA layer is above 35 Å. c) Charge density distribution of OA. d) Geometrically stable configurations of OA@I^-, OA@I_3^-, and OA@I_2 models with correlated adsorption energies.

To reveal the underlying reasons for the formation of the iodine adsorption layer in OA, molecular dynamics (MD) simulations and density functional theory (DFT) calculations were conducted. Figure 3a compares the affinities of water and the OA layer for polyiodide using MD simulation. The corresponding distributions of polyiodide concentration before and after diffusion are provided in Figure 3b. It shows that after 1 fs, the polyiodide diffuses about 5 Å toward the OA layer, demonstrating that polyiodide is strongly attracted to the OA layer rather than water. This is also well confirmed by Figure S11, where OA can effectively adsorb polyiodide from the polyiodide solution. Especially, it is well established that the water and the OA layer have a fine separation, which can prevent the solvation of water molecules on the adsorbed iodine species in the OA layer, thus reducing the undesirable polyiodide shuttling phenomenon effectively.[15] DFT calculations were also performed to gain insight into the underlying mechanisms responsible for the affinity of OA toward iodine species. As illustrated in Figure 3c, the charge-density-difference analysis using colored iso-surfaces suggests that the $–NH_2$ groups in OA are the active sites because of their relatively strong polarization resulting from the lone electron pair of N atom. The binding energy values and corresponding configurations of different iodine species (I^-, I_3^-, and I_2) on OA are also represented in Figure 3d. Apparently, the $–NH_2$ groups, functioning as the active site of OA, exhibit a strong adsorption ability for I^-, I_3^-, and I_2, with adsorption energies of ca. –23.13, –

24.45, and –27.79 kcal mol^{-1}, respectively; this promotes retention of iodine species within the OA layer.

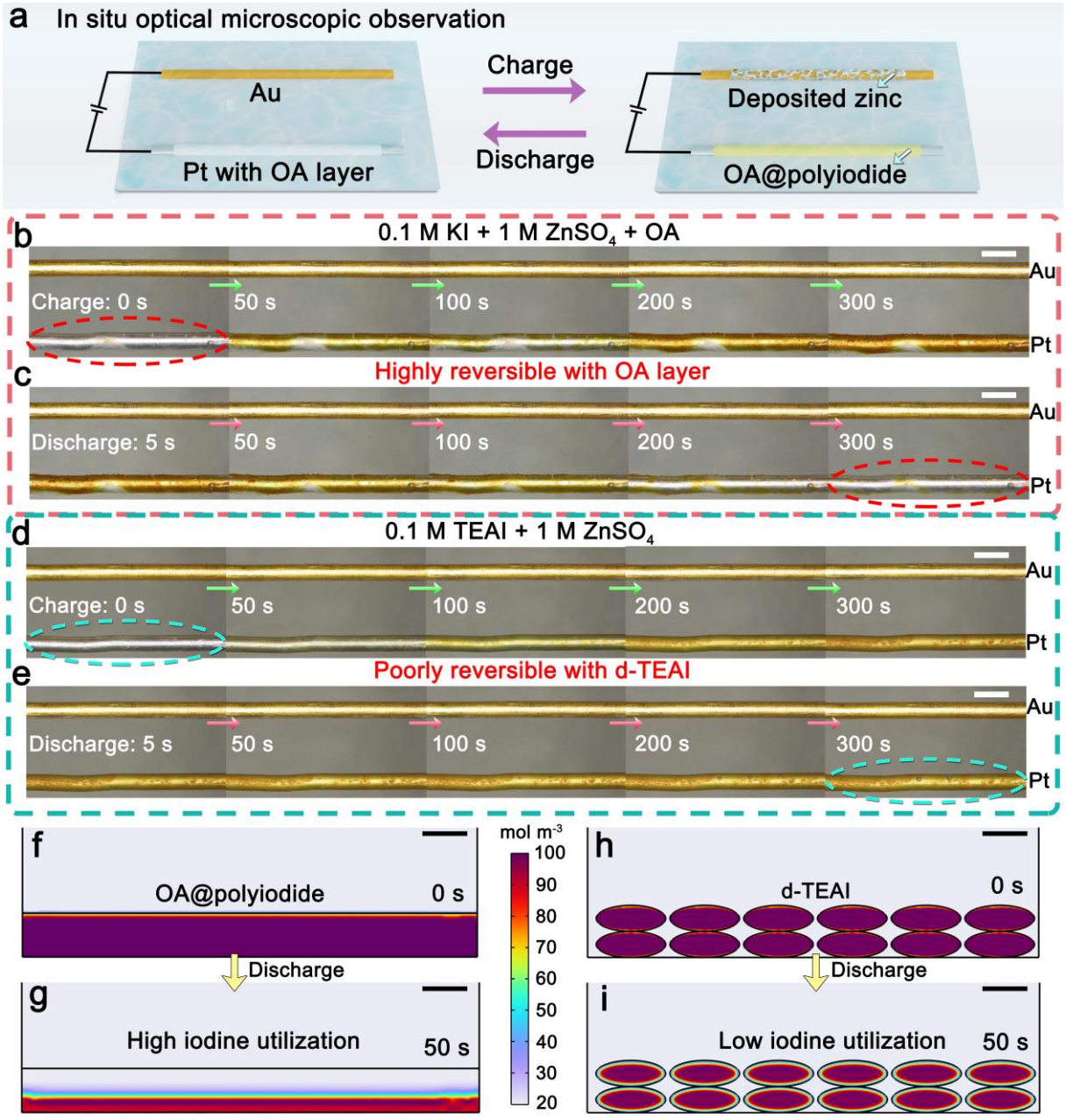

Figure 4. a) Schematic for the observation of iodine conversion process by in-situ optical microscope using Pt with OA layer as the cathode and Au as the anode. Real-time observation of b) oxidation, and c) reduction of iodine species in the OA layer with 1 M $ZnSO_4$ solution containing 0.1 M KI as the electrolyte during charging/discharging at 0.1 mA. Real-time observation of d) oxidation, and e) reduction of iodine species on the Pt electrode with 1 M

$ZnSO_4$ solution containing 0.1 M TEAI as the electrolyte during charging/discharging at 0.1 mA. The scale bar is 1.0 mm. COMSOL Multiphysics simulation for the distribution of the polyiodide concentration within the homogeneous OA layer after discharging for f) 0 s, and g) 50 s at 0.1 A cm^{-2}, and within the stacked d-TEAI layer after discharging for h) 0 s, and i) 50 s at 0.1 A cm^{-2}. The scale bar is 50 μm.

The iodine conversion process within the OA cathode was further visualized using in-situ optical microscopy. Platinum (Pt) and gold (Au) wires with diameters of 0.5 mm are used as the positive and negative current collectors (Figure 4a), receptively.[37] Besides, a thin quasi-solid OA layer is loaded onto the Pt wire as the cathode, along with a 1 M $ZnSO_4$ solution containing 0.1 M KI as the electrolyte. Upon application of a current of 0.1 mA, the initially milky-white OA layer changes rapidly to yellow (Figure 4b), indicating a continuous and rapid oxidation process of I^- ions in the OA layer. With the increase of charging time, the color of the OA layer deepens and demonstrates the ongoing oxidation process. Upon switching to the discharged state after 300 s, thanks to the highly mobile polyiodide ions, the OA layer quickly changes from deep yellow to milky-white again (Figure 4c), signifying the reversible iodine conversion process. Notably, the colorless nature of the electrolyte solution remains unaffected throughout the cycling process. In contrast, without the introduction of an OA layer onto the Pt wire, the highly soluble polyiodide diffuses into the electrolyte, leaving the polyiodide virtually unavailable for reusage during discharging (Figure S12). On another aspect, although d-TEAI shows promise in preserving generated polyiodide in the cathode (Figure 4d), the utilization of polyiodide during discharging in the d-TEAI cathode poses difficulties (Figure 4e). This is because the d-TEAI results in polyiodide being prone to

agglomeration and exhibiting low mobility, making it challenging for polyiodide to engage the current collector for discharge. To provide a clearer illustration, we conducted simulations of the polyiodide reduction process in OA and d-TEAI cathodes using COMSOL Multiphysics software, where the OA with polyiodide (noted as OA@polyiodide) and d-TEAI are represented by a regular rectangle and piled-up ellipses, respectively, based on SEM observations. Meanwhile, the diffusion coefficients of polyiodide are modified to reflect its diffusion behaviors in OA@polyiodide and d-TEAI. When the initial polyiodide concentration is 100 mol m^{-3}, rapid reduction of polyiodide (over half of the polyiodide is reacted within 50 s) occurs in OA@polyiodide at 0.1 A cm^{-2}, demonstrating that a homogeneous layer with fast polyiodide diffusion enables efficient utilization of iodine (Figure 4f&g). However, for d-TEAI, the internal polyiodide remains at a high concentration (>90 mol m^{-3}) after 50 s, while reacting only at the edge. This suggests that the slow diffusion and accumulation of polyiodide is responsible for the low iodine utilization and poor reversibility of d-TEAI electrode (Figure 4h&i). Collectively, these observations provide compelling evidence for the highly reversible, fast, and shuttle-free working mechanism of OA-based ZIBs.

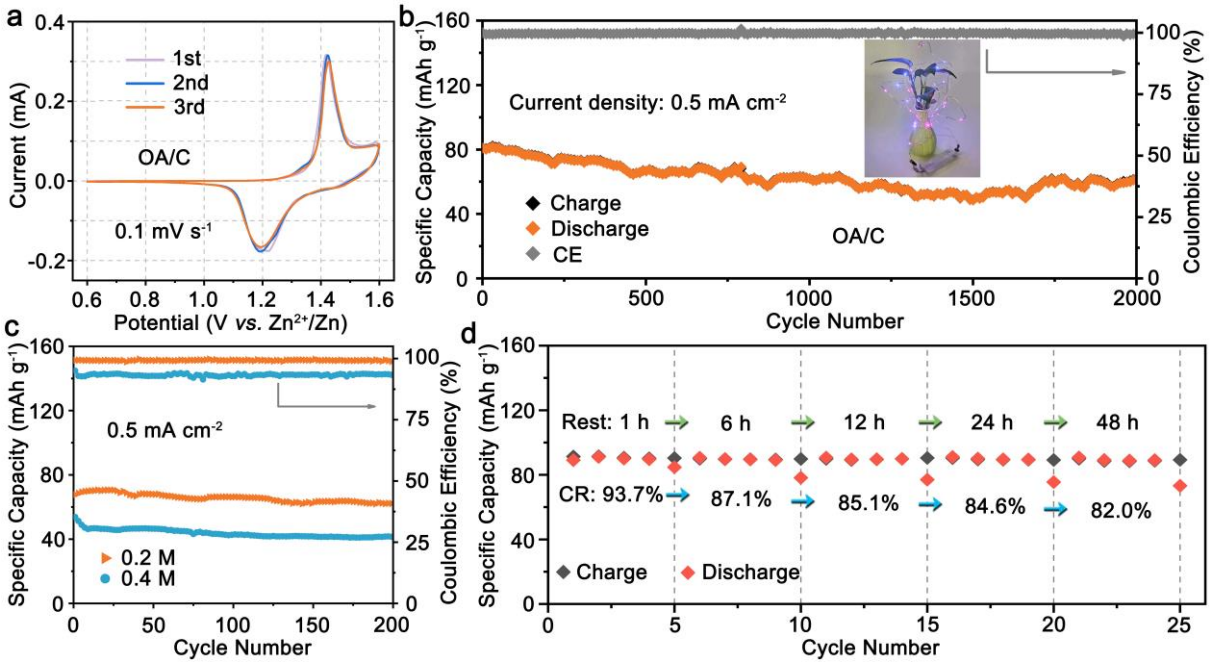

Figure 5. a) CV curves of OA/C-based ZIBs at a scan rate of 0.1 mV s^{-1}. b) Long-term cycling stability performance of OA/C-based ZIBs at 0.5 mA cm^{-2}. Inset shows the use of the as-prepared pouch cell in series to light up the LEDs around the vase. c) Electrochemical performance of OA/C-based ZIBs with electrolytes containing different concentrations of KI at 0.5 mA cm^{-2}. d) Stability performance of OA/C-based ZIBs with different resting times at 0.2 mA cm^{-2}.

The electrochemical properties of the OA/C cathode were further thoroughly investigated in ZIBs. Cyclic voltammetry (CV) curves were collected for OA/C cathode with 0.1 M KI as the iodine source at 0.1 mV s^{-1}. As shown in Figure 5a, the CV curves of the OA/C cathode show a high degree of consistency during the cycling process, demonstrating a high reversibility of iodine redox reaction performed at the OA/C cathode. The charge-discharge voltage profiles of OA/C-based ZIBs at 0.1 mA cm^{-2} are provided in Figure S13**.** Based on the equivalent circuit of electrochemical impedance spectroscopy (Figure S14),[38,39] the cell demonstrates a charge-transfer resistance of ~508 Ω. Additionally, Figure 5b demonstrates the

excellent long-term stability of OA/C-based ZIBs at 0.5 mA cm^{-2}. The cell exhibits a reversible specific capacity of 60.9 mAh g^{-1} (capacity retention: 75.3%) after 2000 cycles, corresponding to an impressive average CE of 99.7%. Besides, it is easily achievable to drive different colors of LED lights around foliage for indoor decoration by a series-connected pouch battery (inset inside Figure 5b), as well as operate for over 60 cycles by a single such cell without capacity loss (Figure S15). These results demonstrate the high competitiveness of OA/C against the iodine hosts with complex preparation processes in Table S1. Besides, the OA/C-based ZIBs using electrolytes containing 0.2 and 0.4 M KI exhibit excellent stabilities after 200 cycles at 0.5 mA cm^{-2}, with capacity retention of 91.0% and 77.1% (Figure 5c), respectively. This outcome suggests that the captured iodine species are effectively confined within OA/C layer. In addition, Figure 5d displays the evaluation of the self-discharge behavior of OA/C-based ZIBs. After resting for different durations (1, 6, 12, 24, and 48 h), the battery exhibits high capacity retention (CR) values of 93.7%, 87.1%, 85.1%, 84.6%, and 82.0%, respectively. Notably, upon recharging after a period of rest, the cell functions properly with ignorable decline in capacity.

In summary, we have successfully developed a novel ZIB cathode based on the heterogeneous LB film formed by the spontaneous spreading of OA/C on the water surface. This method simplifies the cathode fabrication process dramatically, resulting in a preparation time of less than 1 min. Crucially, the as-developed cathode can form a stable and reversible iodine absorption layer due to the following factors: 1) the $-NH_2$ groups in OA can effectively adsorb iodine species; 2) the insoluble property of OA prevents iodine species adsorbed in the OA layer from desolving in water, avoiding the loss of iodine species; 3) the resulting

charge-transfer complexes of $[OA*I^+]I_3^-$, in conjunction with the quasi-solid nature of OA layer, facilitates high mobility and uniform distribution of iodine species within the cathode for fast iodine redox. Therefore, the as-prepared zinc-iodine cells exhibited remarkable cyclability over 2000 cycles, with a capacity retention of 75.3%. This work paves a novel path toward the low-cost and facile preparation of performant iodine cathodes.

ASSOCIATED CONTENT

Supporting Information

The Supporting Information is available free of charge at https://pubs.acs.org/doi/10.1021/acs.nanolett.3c04222

Experimental section; DFT calculations; COMSOL Multiphysics simulations; OM; SEM; XPS; UV-vis; EDS; EIS; GCD curves; ionic conductivity; cycling stability test.

AUTHOR INFORMATION

Corresponding Authors

Feili Lai − Department of Chemistry, KU Leuven, Celestijnenlaan 200F, Leuven 3001, Belgium; State Key Laboratory of Metal Matrix Composites, School of Materials Science and Engineering, Shanghai Jiao Tong University, Shanghai, 200240, P. R. China; ORCID iD: https://orcid.org/0000-0002-4945-0737; E-mail: feili.lai@kuleuven.be and feililai@sjtu.edu.cn

Tianxi Liu − Key Laboratory of Synthetic and Biological Colloids, Ministry of Education, School of Chemical and Material Engineering, International Joint Research Laboratory for

Nano Energy Composites, Jiangnan University, Wuxi, 214122, P. R. China; ORCID iD: http://orcid.org/0000-0002-5592-7386; E-mail: txliu@jiangnan.edu.cn

Authors

Leiqian Zhang: Key Laboratory of Synthetic and Biological Colloids, Ministry of Education, School of Chemical and Material Engineering, International Joint Research Laboratory for Nano Energy Composites, Jiangnan University, Wuxi, 214122, P. R. China

Jiale Ge: Key Laboratory of Synthetic and Biological Colloids, Ministry of Education, School of Chemical and Material Engineering, International Joint Research Laboratory for Nano Energy Composites, Jiangnan University, Wuxi, 214122, P. R. China

Tianlu Wang: Key Laboratory of Synthetic and Biological Colloids, Ministry of Education, School of Chemical and Material Engineering, International Joint Research Laboratory for Nano Energy Composites, Jiangnan University, Wuxi, 214122, P. R. China

Suli Chen: Key Laboratory of Synthetic and Biological Colloids, Ministry of Education, School of Chemical and Material Engineering, International Joint Research Laboratory for Nano Energy Composites, Jiangnan University, Wuxi, 214122, P. R. China; ORCID iD: https://orcid.org/0000-0002-9497-6551

Hele Guo: Department of Chemistry, KU Leuven, Celestijnenlaan 200F, Leuven 3001, Belgium

Elke Debroye: Department of Chemistry, KU Leuven, Celestijnenlaan 200F, Leuven 3001, Belgium; ORCID iD: https://orcid.org/0000-0003-1087-4759

Yue-E Miao: State Key Laboratory for Modification of Chemical Fibers and Polymer Materials, College of Materials Science and Engineering, Donghua University, Shanghai,

201620 P. R. China; ORCID iD: https://orcid.org/0000-0002-3660-029X

Guanjie He: Department of Chemistry, University College London, London, WC1H 0AJ, United Kingdom ; ORCID iD: https://orcid.org/0000-0002-7365-9645

Ivan P. Parkin: Department of Chemistry, University College London, London, WC1H 0AJ, United Kingdom; ORCID iD: https://orcid.org/0000-0002-4072-6610

Johan Hofkens: Department of Chemistry, KU Leuven, Celestijnenlaan 200F, Leuven 3001, Belgium; Department of Molecular Spectroscopy, Max Planck Institute for Polymer Research, Ackermannweg 10, Mainz 55128, Germany; ORCID iD: https://orcid.org/0000-0002-9101-0567

Author Contributions

This manuscript is a joint effort of all the authors.

Notes

The authors declare no competing financial interest.

ACKNOWLEDGMENTS

The authors sincerely acknowledge financial support from the National Natural Science Foundation of China (52161135302 and 52211530489), the Research Foundation-Flanders (1298323N and V404923N), and Shanghai Scientific and Technological Innovation Project (22520710100). J.H. acknowledges financial support from the Research Foundation-Flanders (FWO, Grant Nos. G983.19N, G0F2322N, VS06523N, and ZW15_09-G0H6316N), the Flemish government through long-term structural funding Methusalem (CASAS2, Meth/15/04 and the Moonshot cSBO project P2C (HBC.2019.0108)), Interne Fondsen KU

Leuven through project C3/20/067 and the MPI as an MPI fellow. E.D. acknowledges financial support from the KU Leuven Internal Funds (Grant Numbers STG/21/010, C14/23/090, and CELSA/23/018). We also thank the central laboratory, School of Chemical and Materials Engineering, Jiangnan University for their help in characterization.

REFERENCES

(1) Zhang, Y.; Wang, L.; Li, Q.; Hu, B.; Kang, J.; Meng, Y.; Zhao, Z.; Lu, H. Iodine Promoted Ultralow Zn Nucleation Overpotential and Zn-Rich Cathode for Low-Cost, Fast-Production and High-Energy Density Anode-Free Zn-Iodine Batteries. *Nano-micro Lett.* **2022**, *14* (1), 208.

(2) Du, W.; Ang, E. H.; Yang, Y.; Zhang, Y.; Ye, M.; Li, C. C. Challenges in the Material and Structural Design of Zinc Anode towards High-Performance Aqueous Zinc-Ion Batteries. *Energy Environ. Sci.* **2020**, *13* (10), 3330-3360.

(3) Ruan, P.; Liang, S.; Lu, B.; Fan, H. J.; Zhou, J. Design Strategies for High-Energy-Density Aqueous Zinc Batteries. *Angew. Chem.* **2022**, *134* (17), e202200598.

(4) Luo, M.; Gan, X.; Zhang, C.; Yang, Y.; Yue, W.; Zhitomirsky, I.; Shi, K. Overcoming Obstacles in Zn-Ion Batteries Development: Application of Conductive Redox-Active Polypyrrole/Tiron Anolyte Interphase. *Adv. Funct. Mater.* **2023**, *33* (47), 2305041.

(5) Gan, X.; Tang, J.; Wang, X.; Gong, L.; Zhitomirsky, I.; Qie, L.; Shi, K. Aromatic Additives with Designed Functions Ameliorating Chemo-Mechanical Reliability for Zinc-Ion Batteries. *Energy Storage Mater.* **2023**, *59*, 102769.

(6) Tang, B.; Shan, L.; Liang, S.; Zhou, J. Issues and Opportunities Facing Aqueous Zinc-Ion Batteries. *Energy Environ. Sci.* **2019**, *12* (11), 3288-3304.

(7) He, G.; Parkin, I. P. Sustainable and Biocompatible Zn-based Batteries. *Nat. Sci. Rev.* **2023**, *10* (4), nwad055.

(8) Gan, X.; Zhang, C.; Ye, X.; Qie, L.; Shi, K. Unveiling the Potential of Redox Electrolyte Additives in Enhancing Interfacial Stability for Zn-ion Hybrid Capacitors. *Energy Storage Mater.* **2024**, *65*, 103175.

(9) He, G.; Liu, Y.; Gray, D. E.; Othon, J. Conductive Polymer Composites Cathodes for Rechargeable Aqueous Zn-ion Batteries: A Mini-Review. *Compos. Commun.* **2021**, *27*, 100882.

(10) Subjalearndee, N.; He, N.; Cheng, H.; Tesatchabut, P.; Eiamlamai, P.; Limthongkul, P.; Intasanta, V.; Gao, W.; Zhang, X. Gamma(ɣ)-MnO_2/rGO Fibered Cathode Fabrication from Wet Spinning and Dip Coating Techniques for Cable-Shaped Zn-Ion Batteries. *Adv. Fiber Mater.* **2022**, *4* (3), 457-474.

(11) Wang, Z.; Zhou, M.; Qin, L.; Chen, M.; Chen, Z.; Guo, S.; Wang, L.; Fang, G.; Liang, S. Simultaneous Regulation of Cations and Anions in an Electrolyte for High-Capacity, High-Stability Aqueous Zinc–Vanadium Batteries. *eScience* **2022**, *2* (2), 209-218.

(12) Lin, D.; Li, Y. Recent Advances of Aqueous Rechargeable Zinc-Iodine Batteries: Challenges, Solutions, and Prospects. *Adv. Mater.* **2022**, *34* (23), 2108856.

(13) Yang, S.; Guo, X.; Lv, H.; Han, C.; Chen, A.; Tang, Z.; Li, X.; Zhi, C.; Li, H. Rechargeable Iodine Batteries: Fundamentals, Advances, and Perspectives. *ACS Nano* **2022**, *16* (9), 13554-13572.

(14) Ma, J.; Liu, M.; He, Y.; Zhang, J. Iodine Redox Chemistry in Rechargeable Batteries. *Angew. Chem. Int. Ed.* **2021**, *60* (23), 12636-12647.

(15) Yang, Y.; Liang, S.; Lu, B.; Zhou, J. Eutectic Electrolyte based on N-methylacetamide for Highly Reversible Zinc-Iodine Battery. *Energy Environ. Sci.* **2022**, *15* (3), 1192-1200.

(16) Zhang, L.; Huang, J.; Guo, H.; Ge, L.; Tian, Z.; Zhang, M.; Wang, J.; He, G.; Liu, T.; Hofkens, J.; et al. Tuning Ion Transport at the Anode-Electrolyte Interface via a Sulfonate-Rich Ion-Exchange Layer for Durable Zinc-Iodine Batteries. *Adv. Energy Mater.* **2023**, *13* (13), 2203790.

(17) Ji, Y.; Xie, J.; Shen, Z.; Liu, Y.; Wen, Z.; Luo, L.; Hong, G. Advanced Zinc-Iodine Batteries with Ultrahigh Capacity and Superior Rate Performance Based on Reduced Graphene Oxide and Water-in-Salt Electrolyte. *Adv. Funct. Mater.* **2023**, *33* (10), 2210043.

(18) Zhang, L.; Zhang, M.; Guo, H.; Tian, Z.; Ge, L.; He, G.; Huang, J.; Wang, J.; Liu, T.; Parkin, I. P. A Universal Polyiodide Regulation Using Quaternization Engineering toward High Value-Added and Ultra-Stable Zinc-Iodine Batteries. *Adv. Sci.* **2022**, *9* (13), 2105598.

(19) Liu, M.; Chen, Q.; Cao, X.; Tan, D.; Ma, J.; Zhang, J. Physicochemical Confinement Effect Enables High-Performing Zinc-Iodine Batteries. *J. Am. Chem. Soc.* **2022**, *144* (47), 21683-21691.

(20) Pan, H.; Li, B.; Mei, D.; Nie, Z.; Shao, Y.; Li, G.; Li, X. S.; Han, K. S.; Mueller, K. T.; Sprenkle, V.; Liu, J. Controlling Solid-Liquid Conversion Reactions for a Highly Reversible Aqueous Zinc-Iodine Battery. *ACS Energy Lett.* **2017**, *2* (12), 2674-2680.

(21) Zhang, L.; Guo, H.; Zong, W.; Huang, Y.; Huang, J.; He, G.; Liu, T.; Hofkens, J.; Lai, F. Metal–Iodine Batteries: Achievements, Challenges, and Future. *Energy Environ. Sci.* **2023**, *16*, 4872-4925.

(22) Li, X.; Li, N.; Huang, Z.; Chen, Z.; Liang, G.; Yang, Q.; Li, M.; Zhao, Y.; Ma, L.; Dong, B.; et al. Enhanced Redox Kinetics and Duration of Aqueous I_2/I^- Conversion Chemistry by MXene Confinement. *Adv. Mater.* **2021**, *33* (8), e2006897.

(23) Ma, L.; Ying, Y.; Chen, S.; Huang, Z.; Li, X.; Huang, H.; Zhi, C. Electrocatalytic Iodine Reduction Reaction Enabled by Aqueous Zinc-Iodine Battery with Improved Power and Energy Densities. *Angew. Chem. Int. Ed.* **2021**, *60* (7), 3791-3798.

(24) Bai, X.; Xu, L.; Tang, J. Y.; Zuo, Y. Y.; Hu, G. Adsorption of Phospholipids at the Air-Water Surface. *Biophys. J.* **2019**, *117* (7), 1224-1233.

(25) Miñones, J; Rodríguez Patino, J.M; Conde, O; Carrera, C; Seoane, R. The Effect of Polar Groups on Structural Characteristics of Phospholipid Monolayers Spread at the Air-Water Interface. *Colloid. Surface. A* **2002**, *203* (1-3), 273-286.

(26) Mohwald H. Phospholipid and Phospholipid-Protein Monolayers at the Air/Water Interface. *Annu. Rev. Phys. Chern.* **1990**, *41* (1), 441-476.

(27) Dymond J. H.; O/ye H. A. Viscosity of Selected Liquid n-alkanes. *J. Phys. Chem. Ref. Data* **1994**, *23* (1), 41-53.

(28) Oliveira, O. N. Jr.; Caseli, L.; Ariga, K. The Past and the Future of Langmuir and Langmuir-Blodgett Films. *Chem. Rev.* **2022**, *122* (6), 6459-6513.

(29) Fang, C.; Yoon, I.; Hubble, D.; Tran, T. N.; Kostecki, R.; Liu, G. Recent Applications of Langmuir-Blodgett Technique in Battery Research. *ACS Appl. Mater.* **2022**, *14* (2), 2431-2439.

(30) Sanatkaran, N.; Kulichikhin, V. G.; Malkin, A. Y.; Foudazi, R. Spreading of Oil-in-Water Emulsions on Water Surface. *Langmuir* **2018**, *34* (37), 10974-10983.

(31) Chen, C.; Li, Z.; Xu, Y.; An, Y.; Wu, L.; Sun, Y.; Liao, H.; Zheng, K.; Zhang, X. High-Energy Density Aqueous Zinc-Iodine Batteries with Ultra-long Cycle Life Enabled by the ZnI_2 Additive. *ACS Sustain. Chem. Eng.* **2021**, *9* (39), 13268-13276.

(32) Tran, H.-C. V.; Kim, B.; Kim, H.; Park, S.; Woo, J. Y.; Jeong, S. Unraveling the Role of Triiodides in Halide Precursors for Facile Anion Exchange in Lead Halide Perovskite Nanocrystals. *Chem. Mater.* **2022**, *34* (14), 6402-6407.

(33) Katzin, L. I.; Gebert, E. Solvent Effects in the Iodide-Iodine-Triiodide Complex Equilibrium[1]. *J. Am. Chem. Soc.* **1954**, *76* (8), 2049-2054.

(34) Kim, H.; Kim, K. M.; Ryu, J.; Ki, S.; Sohn, D.; Chae, J.; Chang, J. Triiodide-in-Iodine Networks Stabilized by Quaternary Ammonium Cations as Accelerants for Electrode Kinetics of Iodide Oxidation in Aqueous Media. *ACS Appl. Mater. Interfaces* **2022**, *14* (10), 12168-12179.

(35) Gong, Z.; Song, C.; Bai, C.; Zhao, X.; Luo, Z.; Qi, G.; Liu, X.; Wang, C.; Duan, Y.; Yuan, Z. Anchoring High-mass Iodine to Nanoporous Carbon with Large-Volume Micropores and Rich Pyridine-N Sites for High-Energy-Density and Long-Life Zn-I_2 Aqueous Battery. *Sci. China Mater.* **2023**, *66* (2), 556-566.

(36) Li, Y.; Liu, L.; Li, H.; Cheng, F.; Chen, J. Rechargeable Aqueous Zinc–Iodine Batteries: Pore Confining Mechanism and Flexible Device Application. *ChemComm* **2018**, *54* (50), 6792-6795.

(37) Dai, C.; Hu, L.; Jin, X.; Wang, Y.; Wang, R.; Xiao, Y.; Li, X.; Zhang, X.; Song, L.; Han, Y.; et al. Fast Constructing Polarity-Switchable Zinc-Bromine Microbatteries with High Areal Energy Density. *Sci. Adv.* **2022**, *8* (28), eabo6688.

(38) Zheng, Y.; Ni, X.; Li, K.; Yu, X.; Song, H.; Chen, S.; Khan, N. A.; Wang, D.; Zhang, C. Multi-Heteroatom-Doped Hollow Carbon Nanocages from ZIF-8@CTP Nanocomposites as High-Performance Anodes for Sodium-Ion Batteries. *Compos. Commun.* **2022**, *32*, 101116.

(39) Zhang, S.; Luo, J.; Zhang, F.; He, X. Highly Porous and Thermally Stable Zeolitic Imidazolate Framework-8/Aramid Nanofibers Composite Separator for Lithium-Ion Batteries. *Compos. Commun.* **2022**, *32*, 101183.